Langmuir Article

pubs.acs.org/Langmuir

Superhydrophobic and Superoleophobic Nanocellulose Aerogel Membranes as Bioinspired Cargo Carriers on Water and Oil

Hua Jin,[†] Marjo Kettunen,[†,⊥] Ari Laiho,[†,∥] Hanna Pynnönen,[‡] Jouni Paltakari,[‡] Abraham Marmur,[§] Olli Ikkala,*[,†] and Robin H. A. Ras*[,†]

[†]*Molecular Materials, Department of Applied Physics, Helsinki University of Technology/Aalto University, Puumiehenkuja 2, FIN-02150 Espoo, Finland,* [‡]*Forest Products Technology, Helsinki University of Technology/Aalto University, Tekniikantie 3, FIN-02150 Espoo, Finland, and* [§]*Department of Chemical Engineering, Technion - Israel Institute of Technology, 32000 Haifa, Israel.* [∥]*Present address: Department of Science and Technology, Organic Electronics, Linköping University, SE-601 74, Norrköping, Sweden.* [⊥]*Marjo Kettunen née Marjo Pääkkö*

Received September 27, 2010. Revised Manuscript Received December 15, 2010

We demonstrate that superhydrophobic and superoleophobic nanocellulose aerogels, consisting of fibrillar networks and aggregates with structures at different length scales, support considerable load on a water surface and also on oils as inspired by floatation of insects on water due to their superhydrophobic legs. The aerogel is capable of supporting a weight nearly 3 orders of magnitude larger than the weight of the aerogel itself. The load support is achieved by surface tension acting at different length scales: at the macroscopic scale along the perimeter of the carrier, and at the microscopic scale along the cellulose nanofibers by preventing soaking of the aerogel thus ensuring buoyancy. Furthermore, we demonstrate high-adhesive pinning of water and oil droplets, gas permeability, light reflection at the plastron in water and oil, and viscous drag reduction of the fluorinated aerogel in contact with oil. We foresee applications including buoyant, gas permeable, dirt-repellent coatings for miniature sensors and other devices floating on generic liquid surfaces.

1. Introduction

Several plants and animals incorporate superhydrophobic surfaces having a water contact angle CA > 150°, thus providing materials scientists exciting models for functional bioinspired surfaces.[1−4] Classic examples are the self-cleaning leaves of the lotus plant, the nonfogging compound eyes of mosquitoes, and the locomotion of water striders on water surfaces.[1−8] Although a wealth of bioinspired concepts have been introduced to achieve superhydrophobicity,[1−9] superoleophobic surfaces with CA > 150° for oils are rare and considerably more challenging to construct as the surface tension of oils is only a fraction of that of water.[10−15] In addition to chemical composition and roughened texture, a third parameter is essential to achieve superoleophobicity, namely, re-entrant surface curvature in the form of overhang structures. The overhangs can be realized as fibers,[10,12−14] mushroom-like structures,[10] and pores.[11,16] Superoleophobic surfaces are appealing for, for example, antifouling, since purely superhydrophobic surfaces are easily contaminated by oily substances in practical applications, which in turn will impair the liquid repellency.

Whereas bioinspired floating on water is demonstrated using superhydrophobic surfaces,[17−24] no concepts have been shown for floating and load bearing on oily liquids based on superoleophobicity. This could be conceptually interesting for, for example, autonomous devices sensing pollution on water or other chemical environments.

The aerogel used in current work is an ultralightweight solid material composed of native cellulose nanofibers.[25] The 10−20 nm native cellulose nanofibers are cleaved from the self-assembled hierarchy of macroscopic cellulose fibers.[26] They have become highly topical, as they are proposed to show extraordinary mechanical properties due to their parallel and grossly hydrogen bonded polysaccharide chains.[27] A very high tensile modulus of

*To whom correspondence should be addressed. E-mail: robin.ras@tkk.fi (R.H.A.R.); olli.ikkala@tkk.fi (O.I.). Fax: +358-9-470 23155.

(1) Xia, F.; Jiang, L. *Adv. Mater.* **2008**, *20*, 2842.
(2) Zhang, X.; Shi, F.; Niu, J.; Jiang, Y.; Wang, Z. *J. Mater. Chem.* **2008**, *18*, 621.
(3) Genzer, J.; Marmur, A. *MRS Bull.* **2008**, *33*, 742.
(4) Liu, M.; Zheng, Y.; Zhai, J.; Jiang, L. *Acc. Chem. Res.* **2010**, *43*, 368.
(5) Quéré, D. *Annu. Rev. Mater. Res.* **2008**, *38*, 71.
(6) Bush, J. W. M.; Hu, D. L. *Annu. Rev. Fluid Mech.* **2006**, *38*, 339.
(7) Shi, F.; Niu, J.; Liu, J.; Liu, F.; Wang, Z.; Feng, X.-Q.; Zhang, X. *Adv. Mater.* **2007**, *19*, 2257.
(8) Feng, X. Q.; Gao, X. F.; Wu, Z. N.; Jiang, L.; Zheng, Q. S. *Langmuir* **2007**, *23*, 4892.
(9) Li, S. H.; Zhang, S. B.; Wang, X. H. *Langmuir* **2008**, *24*, 5585.
(10) Tuteja, A.; Choi, W.; Ma, M.; Mabry, J. M.; Mazzella, S. A.; Rutledge, G. C.; McKinley, G. H.; Cohen, R. E. *Science* **2007**, *318*, 1618.
(11) Steele, A.; Bayer, I.; Loth, E. *Nano Lett.* **2009**, *9*, 501.
(12) Leng, B. X.; Shao, Z. Z.; de With, G.; Ming, W. H. *Langmuir* **2009**, *25*, 2456.
(13) Jin, H.; Pääkkö, M.; Ikkala, O.; Ras, R. H. A. Liquid-repellent material. Patent Application FI 20095752, PCT/FI2010/050575, July 2, 2009.
(14) Aulin, C.; Netrval, J.; Wågberg, L.; Lindström, T. *Soft Matter* **2010**, *6*, 3298.
(15) Marmur, A. *Langmuir* **2008**, *24*, 7573.
(16) Cao, L. L.; Price, T. P.; Weiss, M.; Gao, D. *Langmuir* **2008**, *24*, 1640.
(17) Pan, Q. M.; Wang, M. *ACS Appl. Mater. Interfaces* **2009**, *1*, 420.
(18) Pan, Q. M.; Liu, J.; Zhu, Q. *ACS Appl. Mater. Interfaces* **2010**, *2*, 2026.
(19) Jiang, Z. X.; Geng, L.; Huang, Y. D. *J. Phys. Chem. C* **2010**, *114*, 9370.
(20) Zhao, Y.; Tang, Y. W.; Wang, X. G.; Lin, T. *Appl. Surf. Sci.* **2010**, *256*, 6736.
(21) Larmour, I. A.; Bell, S. E. J.; Saunders, G. C. *Angew. Chem., Int. Ed.* **2007**, *46*, 1710.
(22) Liu, J. L.; Feng, X. Q.; Wang, G. F. *Phys. Rev. E* **2007**, *76*, 066103.
(23) Chen, X.; Gao, J.; Song, B.; Smet, M.; Zhang, X. *Langmuir* **2010**, *26*, 104.
(24) Bormashenko, E.; Bormashenko, Y.; Musin, A. *J. Colloid Interface Sci.* **2009**, *333*, 419.
(25) Pääkkö, M.; Vapaavuori, J.; Silvennoinen, R.; Kosonen, H.; Ankerfors, M.; Lindström, T.; Berglund, L. A.; Ikkala, O. *Soft Matter* **2008**, *4*, 2492.
(26) Pääkkö, M.; Ankerfors, M.; Kosonen, H.; Nykänen, A.; Ahola, S.; Österberg, M.; Ruokolainen, J.; Laine, J.; Larsson, P. T.; Ikkala, O.; Lindström, T. *Biomacromolecules* **2007**, *8*, 1934.
(27) Henriksson, M.; Berglund, L. A.; Isaksson, P.; Lindström, T.; Nishino, T. *Biomacromolecules* **2008**, *9*, 1579.

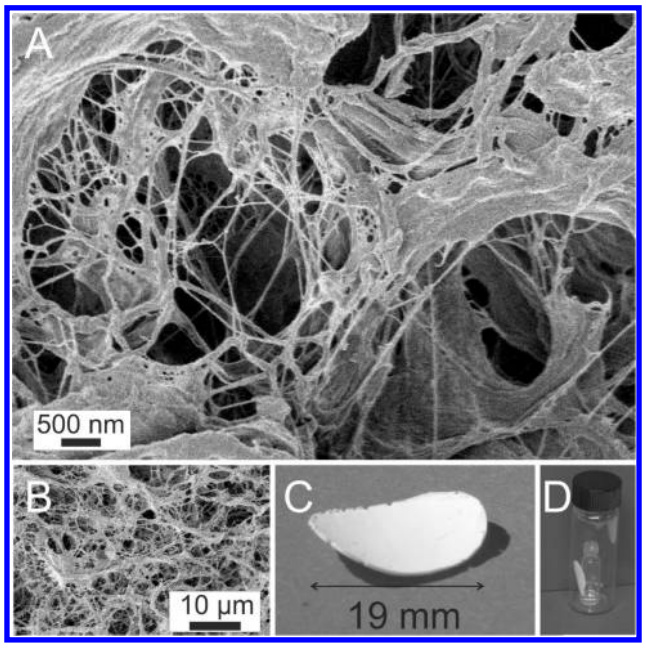

Figure 1. (A,B) Scanning electron micrographs of native nanocellulose aerogel structure with robust network structuring at several length scales due to individual nanofibers and their aggregates. (C) Photograph of a nanocellulose aerogel membrane. (D) Bottle-in-bottle setup for fluorination by chemical vapor deposition.

ca. 150 GPa has already been shown.[28] The concepts based on nanocellulose may well turn out to allow a new paradigm for superstrong biological fibers in addition to silk.[29] Upon cleaving, the cellulose nanofibers form aqueous hydrogels, and a subsequent freeze-drying leads to highly porous aerogels (Figure 1).[25,30] Previously we have demonstrated two different freeze-drying methods for cellulose aerogels: cryogenic freeze-drying and vacuum freeze-drying.[25] In the cryogenic freeze-drying method, the hydrogel is frozen by immersion in a cryogenic liquid, followed by water removal by sublimation in vacuum. The state of aggregation can be controlled qualitatively: quicker cooling in freeze-drying leads to smaller aggregates.[25] In the vacuum freeze-drying method, the hydrogel is placed in a vacuum chamber and then it cools down and freezes due to the evaporation process, followed by sublimation. During the vacuum freeze-drying process, some aggregation of the cellulose nanofibers takes place (see Figure 1A, B). In addition to the freeze-drying conditions, also the solids content of the hydrogel affects the structure and the internal surface area of the aerogel.[31] Unlike most aerogels, the native nanocellulose aerogels are not brittle.[25,32]

Superoleophobic nanocellulose aerogels have recently been achieved using unmodified cellulose nanofibers[13] and using carboxymethylated, negatively charged cellulose nanofibers[14] as starting materials. In this work, the aerogels made from unmodified cellulose nanofibers were subsequently treated with fluorosilanes. To complement previous work on superoleophobic aerogels, we demonstrate their application as cargo carriers on water and oil, gas permeability, plastrons, and drag reduction, and we show that fluorinated nanocellulose aerogels are high-adhesive superhydrophobic and high-adhesive superoleophobic surfaces.

2. Experimental Section

Preparation of Hydrogels of Native Cellulose Nanofibers. The pulp used in refining to access native cellulose nanofibers was a commercial never-dried ECF-bleached birch kraft pulp from UPM-Kymmene, Finland. The pulp suspension was at first diluted to 3% consistency, and cellulose nanofibers were disintegrated using an ultrafine friction grinder (Masuko Supermass-colloider, model MKZA 10-15J). The grinder consists of lower rotating and upper stationary SiC grinding stones (gap 100 μm). During the grinding, the power consumption was kept at levels 3.2−3.8 kW (total energy consumed 15 kWh/t). Pulp suspension was recirculated into the grinder five times. The grinding leads to hydrogels due to disintegration of the macroscopic cellulose fibers into nanofibers. The Masuko method of cleaving results in nanofibers with comparable microscopic structure as nanofibers obtained using microfluidization method.[26] Water was added during the grinding process, leading to a nanocellulose hydrogel with a final solids content of 1.3%. The contamination from the grinding stones is negligible.

Preparation of Aerogel Membranes. Drying of native nanocellulose hydrogels into aerogel membranes without essential collapse has been described before.[25] In order to make the nanofibers well dispersed, the hydrogel was magnetically stirred for 1 day before use. The mold used to prepare the aerogel membranes was a press-to-seal silicone isolator (Grace Bio-Laboratories, thickness of 0.5 mm, diameter of 20 mm) on a glass slide. The mold was carefully filled with the nanocellulose hydrogel. Next, the mold with hydrogel was transferred in a vacuum oven at room temperature. When the hydrogel sample was exposed to vacuum, it quickly became frozen and the sample was then dried by sublimation in the vacuum oven. The drying was stopped when the pressure reached 3×10^{-2} mbar.

Fluorination of the Aerogel Membranes by Chemical Vapor Deposition (CVD). A piece of the aerogel membrane (Figure 1C) was placed in a 30 mL glass bottle. A total of 200 μL of (tridecafluoro-1,1,2,2-tetrahydrooctyl)trichlorosilane (FTCS) (97%, ABCR) was inserted in another 2 mL glass bottle. The 2 mL glass bottle containing FTCS was placed inside the above-mentioned 30 mL bottle (see Figure 1D). This "bottle-in-bottle" setup was designed to avoid direct contact between the aerogel membrane and liquid FTCS. Finally, the 30 mL bottle was sealed with a cap and placed for 2 h in an oven at 70 °C. To remove the unreacted silanes, the aerogel was kept in a vacuum oven until the vacuum level reached 3×10^{-2} mbar or less. Other fluorinated silanes such as (bis(tridecafluoro-1,1,2,2-tetrahydrooctyl)dimethylsiloxy)-methylchlorosilane, (tridecafluoro-1,1,2,2-tetrahydrooctyl)dimethylchlorosilane, and (heptadecafluoro-1,1,2,2-tetrahydrodecyl)dimethylchlorosilane were tested under the same reaction conditions.

Scanning Electron Microscopy (SEM). A JEOL JSM-7500F field emission scanning electron microscope (FE-SEM) was used to characterize the nanostructures and to observe the porosity in nanocellulose aerogel membranes. In order to avoid charging, the membranes were sputtered with gold under vacuum conditions at 20 mA for 1 min.

Contact Angle Measurement. The wetting properties of the aerogel membranes were characterized by using a CAM 200 Optical contact angle meter (KSV Instruments). In the static mode, droplets of Milli-Q water, paraffin oil (University Pharmacy Ltd.; Finland, used as received), or mineral oil (Teresstic, grade ISOV6150, used as received) were placed on the surface of the fluorinated membrane at room temperature. The droplet volume for water was 10 μL and for oils 5 μL. The contact angle values were calculated using the contact angle meter software

(28) Iwamoto, S.; Kai, W.; Isogai, A.; Iwata, T. *Biomacromolecules* **2009**, *10*, 2571.
(29) Meyers, M. A.; Chen, P.-Y.; Lin, A. Y.-M.; Seki, Y. *Prog. Mater. Science* **2008**, *53*, 1.
(30) Ikkala, O.; Ras, R. H. A.; Houbenov, N.; Ruokolainen, J.; Pääkkö, M.; Laine, J.; Leskelä, M.; Berglund, L. A.; Lindström, T.; ten Brinke, G.; Iatrou, H.; Hadjichristidis, N.; Faul, C. F. J. *Faraday Discuss.* **2009**, *143*, 95.
(31) Jin, H.-J.; Nishiyama, Y.; Wada, M.; Kuga, S. *Colloids Surf., A* **2004**, *240*, 63.
(32) Olsson, R. T.; Samir, M. A. S. A.; Salazar-Alvarez, G.; Belova, L.; Strom, V.; Berglund, L. A.; Ikkala, O.; Nogues, J.; Gedde, U. W. *Nature Nanotech.* **2010**, *5*, 584.

based on the shape of the droplet in the image. Contact angle values for both water and oil were recorded for 2 min and remained stable. To obtain further information about the wetting properties, images were taken when the fluorinated aerogel surface was tilted at 90° and 180° for both water and oil. The droplets at these angles remained stable during the 2 min measurement.

Load Carrying Experiment. A fluorinated aerogel membrane with diameter of 19 mm, thickness of 0.5 mm, and mass of 3.0 mg was placed on a bath filled with Milli-Q water or filled with paraffin oil. A ruler was placed parallel to the bath. Loads were carefully added on top of the aerogel membrane. The total mass of the weights before the aerogel sank was measured. Contrast illumination allowed imaging the meniscus of the dimple.

Light Reflection. A piece of fluorinated aerogel membrane was immersed in water and paraffin oil. Metallic appearance due to light reflection indicates the presence of the plastron. In order to check the stability of plastrons in both water and oil, the samples were kept immersed for 1 week. In another setup, a red laser beam was reflected on the surface of the fluorinated aerogel when it was immersed in water. The reflected light was collected on a white screen.

Drag Reduction Experiment. A shear stress controlled Bohlin CS50 rheometer with stainless steel cone/plate geometry (40 mm diameter and 4° cone angle) was used to study the viscous drag reduction at the surface of the fluorinated aerogel membrane. The fluorinated aerogel membrane was attached to the bottom plate of the rheometer with double-sided Scotch tape, and thereafter a layer of silicone oil (Sigma-Aldrich, 1 Pa·s) was placed between the membrane and the metal cone. The shear stress was measured as a function of shear rate.

3. Results and Discussion

Mechanically robust nanocellulose aerogels with a mass of 3.0 mg, diameter of 19 mm, and thickness of 0.5 mm are prepared by vacuum freeze-drying. The resulting density is 0.02 g/cm^3. Taking the definition of porosity $\phi = 1 - (\rho_a/\rho_s)$, where ρ_a is the density of aerogel and ρ_s is the density of crystalline cellulose (1.5 g/cm^3),[33] the resulting porosity is 98.6%. The aerogels were fluorinated with fluorosilanes using chemical vapor deposition (CVD) (see Figure 1D for the bottle-in-bottle setup for CVD).[4,13,14] The unmodified aerogel contains free hydroxyl groups on the surface, which react with chlorosilanes to form a covalent Si−O bond. Different fluorinated chlorosilanes were tested under same reaction conditions (see Supporting Information, Table S1). FTCS gives the highest contact angle with water, and it was used for all other experiments. From the Si elemental analysis combined with Brunauer−Emmett−Teller (BET) specific surface area, we obtain a FTCS molecular area of 0.50 nm^2, which corresponds to a dense FTCS monolayer (see the Supporting Information). There are two advantages of the CVD bottle-in-bottle setup. First, it avoids direct contact of the aerogel with the liquid fluorosilane. Second, it reacts at low temperature (70 °C) so that the inherent structures and properties of cellulose aerogel do not get damaged and the aerogel remains white. Without the fluorination treatment, a water droplet becomes immediately absorbed within an aerogel without any measurable contact angle. Figure S1A in the Supporting Information demonstrates that a drop of aqueous methylene green ink gets readily absorbed by the native nanocellulose aerogel, making it colored. The methylene green dye is so strongly bonded to the cellulose surface that it cannot be removed after a washing step, and instead the aerogel disintegrates (Supporting Information, Figure S1B). The native cellulose aerogel is not stable in water, where it swells and falls apart (Supporting Information, Figure S1E). By contrast, for the fluorinated aerogel, a water contact angle of 160° is observed (Figure 2D), indicating superhydrophobicity. The fluorinated aerogel is a high-adhesive superhydrophobic surface,[4] as is evident from the pinning of the droplet at tilted angle (Supporting Information, Figure S2A,B). A drop of methylene green ink on the fluorinated aerogel forms a round droplet and is removed easily (Supporting Information, Figure S1C,D). Furthermore, the fluorinated aerogel is stable in water and remains intact even after exposure for 24 h (Supporting Information, Figure S1F).

Even more interestingly, high contact angles of 153° and 158° are observed for, respectively, paraffin oil and mineral oil (Figure 2C and Supporting Information, Figure S3), indicating additional superoleophobicity. The aerogel is a high-adhesive superoleophobic surface,[4] as the oil droplets remain pinned at tilted angles (Supporting Information, Figure S2C,D). Overhang structures promote superoleophobicity,[10] and the aerogel made from cellulose nanofibers allows a particularly simple and scalable approach for them.[13,14] The mechanism for high-adhesive pinning of the droplets on the cellulose aerogels is not yet clear. Note that the floatation capability of nanostructured aerogel membranes was inspired by the structures at different length scales within the water strider legs, which contain micrometer-sized fibrils (i.e., setae) and nanosized grooves that trap air due to biological surface active coatings and correspondingly the superhydrophobicity (Figure 2A).[34] In a rough analogy, our nanocellulose membranes show structures at several length scales, but in this case the fibrils form networks from nanometer scale individual nanofibers up to micrometer scale nanofibrous aggregates (Figure 2B). Sooner than mimicking the setae that are connected at only one end to the water strider leg, which could suffer brittleness in applications, we incorporate networks of fibers that are expected to be more robust.

The load carrying capabilities on oil and water were inspected (Figure 2C,D). On oil, an aerogel with a mass of 3.0 mg and diameter 19 mm could carry a load of 960 mg, and made a dimple of 2.7 mm depth without sinking. Correspondingly, on water, the aerogel could carry a load of 1658 mg with a dimple of 3.7 mm. Note that under load the water surface is deformed to such a large extent that the complete aerogel and all the metal weights are located below the free liquid surface. The aerogel is thus capable of supporting a weight nearly 3 orders of magnitude larger than the weight of the aerogel itself. The experimental maximum depth of the dimple in water and oil corresponds well with the maximum dimple depth obtained from the theoretical force balance analysis of the floatation of a nanofibers raft.[35] The surface tension acts on the aerogel carrier at different length scales: along the perimeter of the disk, and along each fibril preventing the liquid from penetrating the aerogel, thus maintaining the buoyancy.[35]

The cellulose aerogel is a solid material with an open porous network structure as is shown in Figure 1A and allows permeation of gases. We demonstrate the gas permeability by using a pH indicator paper (Figure 3). Here we encapsulate the indicator paper between fluorinated aerogel membranes and expose it to a vapor of HCl. The pH indicator paper rapidly changes color, which demonstrates that HCl vapor has diffused through the aerogel. The aerogel thus acts as a membrane that is permeable for gases and vapors but impermeable for liquids. We expect this to be relevant for several membrane-based applications.

(33) Eichhorn, S. J.; Dufresne, A.; Aranguren, M.; Marcovich, N. E.; Capadona, J. R.; Rowan, S. J.; Weder, C.; Thielemans, W.; Roman, M.; Renneckar, S.; Gindl, W.; Veigel, S.; Keckes, J.; Yano, H.; Abe, K.; Nogi, M.; Nakagaito, A. N.; Mangalam, A.; Simonsen, J.; Benight, A. S.; Bismarck, A.; Berglund, L. A.; Peijs, T. *J. Mater. Sci.* **2010**, *45*, 1.

(34) Gao, X.; Jiang, L. *Nature* **2004**, *432*, 36.

(35) Marmur, A.; Ras, R. H. A. Unpublished work.

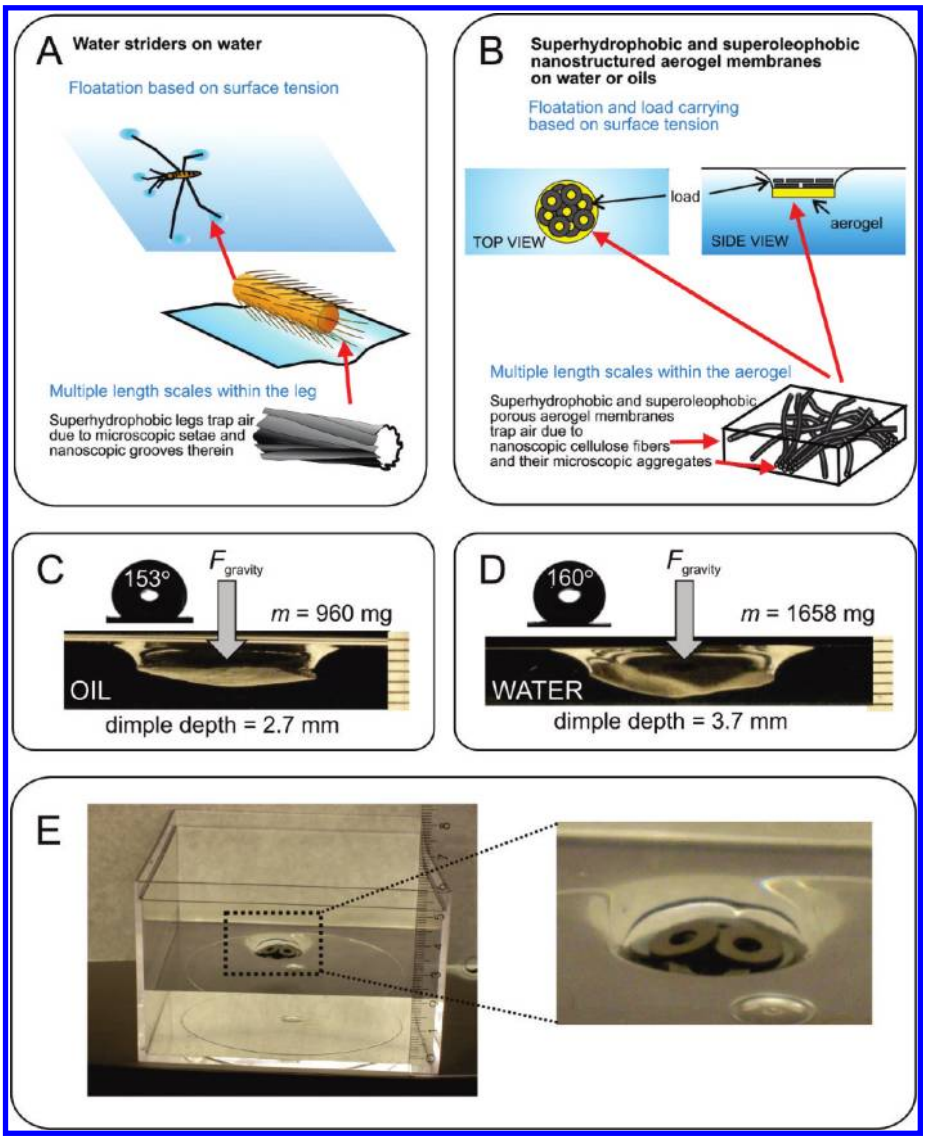

Figure 2. Floatation and load carrying on oil and water based on fluorinated nanostructured aerogel. (A) Inspiration came from water striders, a class of insects capable of floating on water based on surface tension, using superhydrophobic legs with fibrillar structures.[34] (B) Cartoon of a fluorinated nanofibrous cellulose aerogel membrane floating on water and oil due to surface tension. As in water striders, also in the aerogels the topography for liquid repellency is induced by fibers, but in this case the fibers form mechanically robust entangled networks. (C,D) Contact angle measurement and load carrying experiment of the aerogel on, respectively, paraffin oil and water. The side-view photograph of the aerogel load carrier on paraffin oil and water shows the dimple at maximum supportable weight. The scale markers on the right are in millimeters. (E) Load carrying setup. Metal weights (washers) are loaded on the fluorinated aerogel membrane floating on water (similarly on oil).

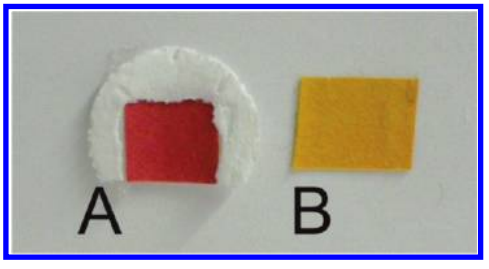

Figure 3. Gas permeability of the fluorinated aerogel membrane. (A) A piece of pH indicator paper is encapsulated between two fluorinated aerogel membranes and subsequently exposed to HCl vapor. Upon exposure, the pH indicator rapidly changes from yellow to red (in the photograph, we removed one aerogel membrane for clarity), showing that HCl vapor rapidly passes through the aerogel. (B) The original pH indicator paper.

When a superhydrophobic material is immersed in water, it may trap a thin layer of air to avoid direct contact between the surface and water.[21,36,37] This layer of air is called a plastron, and it changes the appearance of the surface as light reflects efficiently at the air−water interface. Also the fluorinated aerogel immersed in water has a plastron, seen from the metallic appearance (Supporting Information, Figure S4B). In addition, the fluorinated aerogel shows the plastron also when immersed in oil (Supporting Information, Figure S4A). To the best of our knowledge, this is the first report on a plastron in a solvent different from water. It has to be noted that the plastrons can be observed even after 1 week of immersion, which indicates long-term

(36) Bush, J. W. M.; Hub, D. L.; Prakash, M. *J. Adv. Insect Physiol.* **2008**, *34*, 118.
(37) Zimmermann, J.; Reifler, F. A.; Fortunato, G.; Gerhardt, L. C.; Seeger, S. *Adv. Funct. Mater.* **2008**, *18*, 3662.

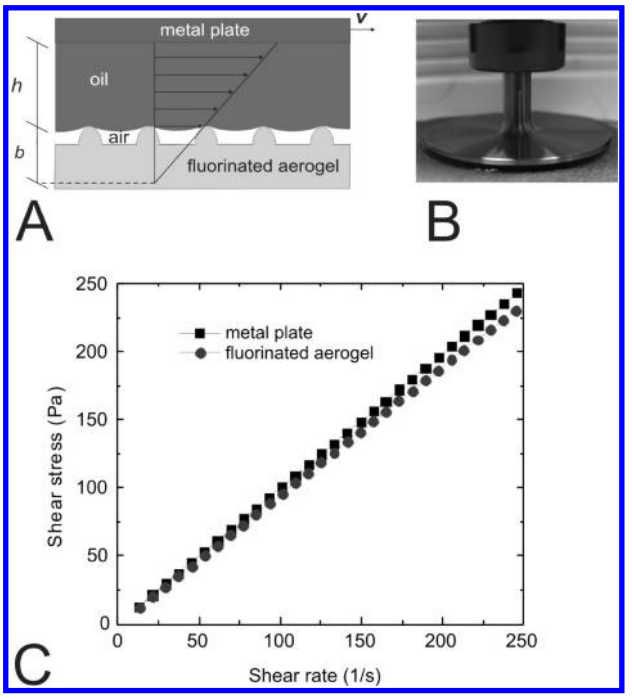

Figure 4. (A) Schematic representation of drag reduction of oil in contact with a superoleophobic surface. The metal plate is at a distance h from the aerogel surface. The slip length b is the distance between the border of the oil and an imaginary point inside the material at which the velocity profile goes to zero. (B) Photograph of the experimental setup. (C) Shear stress versus shear rate curve of a metal−metal cone−plate system (black squares) and a metal−aerogel cone−plate system (gray spheres).

stability of the plastrons in both water and oil. Moreover, the reflection of light at the plastron of a fluorinated aerogel immersed in water was also observed in a different setup using laser light and a white screen (Supporting Information, Figure S5).

We further point out that the aerogel membrane allows slightly reduced viscous drag due to superoleophobicity. Reduced viscous drag of superhydrophobic surfaces in water is a well-known phenomenon, and it finds its origin in the plastron that reduces the direct contact of water to the surface.[38] Recently, a theoretical study on the friction of oils on superoleophobic surfaces was presented.[39] Here, we demonstrate to the best of our knowledge the first experimental evidence of reduced friction at superoleophobic surfaces, giving rise to an effective wall slip that leads to measurable drag reduction in oil flow (Figure 4). We used a silicone oil (Sigma-Aldrich, 1 Pa·s) which had a contact angle of 153° with the superoleophobic aerogel. When compared to the metal−metal cone−plate system, the shear stress τ at the fluorinated aerogel surface is reduced by 5−6%, which corresponds to a considerable slip length of roughly 50 μm.[38,40] The slip length b was calculated based on ref 40:

$$b = \frac{R\theta_0}{4}\left(1 - \sqrt{\frac{8\theta_0}{\pi\Omega R^3}\frac{M}{\mu} - \frac{13}{3}}\right)$$

where R and θ_0 are the cone radius and angle, respectively, $\Omega \approx \theta_0\dot{\gamma}$ is the angular velocity, μ is the viscosity of the oil, and $M \approx (2\pi R^3/3)\tau$ is the torque on the cone.

4. Conclusion

In conclusion, we have demonstrated that the nanocellulose aerogel carrier has some common features with the water strider: load carrying on water, superhydrophobicity, structures ranging from the nanoscale to the micrometer scale, plastron in water, that is, a thin layer of air at the surface of the immersed aerogel, and flexibility. Importantly, the aerogel has additional attractive features including superoleophobicity, load carrying on oil, plastron in oil, and reduced viscous drag. It is also demonstrated that the load carrying capacity may be a few orders of magnitude larger than the weight of the aerogel itself. This opens up a new platform for carriers or for coatings that have large load bearing capability on various organic and aqueous liquids including oil-polluted water. Concomitantly, these carriers are foul-resistant and gas permeable membranes, applicable, for example, as coatings for miniaturized robots or future environmental gas sensors floating on practical liquids.

Acknowledgment. This research was supported by Finnish National Technology Agency (TEKES), UPM-Kymmene, Nokia, Ahlstrom, Ecopulp, Glykos, Elastopoli, Sinebrychoff, Kareline, Dynea, and Teknos within the NASEVA project. This work made use of facilities from the Nanomicroscopy Center (Aalto University).

Supporting Information Available: Additonal table and figures. This material is available free of charge via the Internet at http://pubs.acs.org.

(38) Bocquet, L.; Barrat, J. L. *Soft Matter* **2007**, *3*, 685.
(39) Joly, L.; Biben, T. *Soft Matter* **2009**, *5*, 2549.
(40) Choi, C. H.; Kim, C. J. *Phys. Rev. Lett.* **2006**, *96*, 066001.